academicJournals

Vol. 11(16), pp. 209-216, 30 August, 2016
DOI: 10.5897/IJPS2016.4530
Article Number: A40898B60312
ISSN 1992 - 1950

http://www.academicjournals.org/IJPS

International Journal of Physical Sciences

Full Length Research Paper

Mineral determination and radiological risk caused by geological formations from Iron Ore in Wadi Sawawin, Duba, Saudi Arabia

Alharbi W. R.

Department of Physics, Faculty of Science, King Abdulaziz University, Jeddah, Saudi Arabia.

Received 4 July, 2016; Accepted 16 August, 2016

Fifteen iron ore samples collected from Wadi Sawawin, Duba, Saudi Arabia were analysed using X-ray diffraction in order to determine mineral composition. Atomic absorption analysis was used to determine concentrations of Al, Ca, Fe, K, Mg, Bi, Pb, Th and U. Natural radioactivity concentrations were determined using gamma-ray spectrometry based on a hyper pure germanium (HPGe) detector; concentrations ranged from 1.89±0.39 to 4.50±0.53 Bq kg^{-1}, 1.21±0.16 to 3.60±0.56 Bq kg^{-1} and detection level to 10.33±1.32 Bq kg^{-1} for ^{226}Ra, ^{232}Th and ^{40}K, respectively. In order to assess the potential radiological risks to human health, the absorbed dose rate, radium equivalent activity, annual absorbed dose and external hazards were determined and compared to limits recommended by UNSCEAR. Results were within recommended safe ranges, meaning that the area under study is radiologically safe for habitation and that local iron ores are radiologically safe to be used as construction materials.

Key words: Atomic absorption spectrometer, natural radioactivity, radiological hazard, X-ray powder diffraction (XRD).

INTRODUCTION

Raw materials have emerged as being a key factor in the industrial growth of Wadi Sawawin, in the Duba region of Saudi Arabia, along with agriculture and tourism. Wadi Sawawin is located at 28°02'26.49" North, 360°02'19.48" East, 45 km northeast of Duba, Tabuk Province, Saudi Arabia. The northern region of Duba is the location of the largest iron mine in Saudi Arabia, the Wadi Sawawin mine. This mine is comprised of a vast industrial complex where millions of tons of iron ore are produced annually; the reserve annual production of this mine is estimated to be greater than 500 million tonnes. Duba is an international crossing point, being one of the most important geographical connections between not only the southern and western regions of Duba, but also between the Eastern Province of Saudi Arabia and neighbouring countries. Figure 1 shows the location where samples were collected for this study. Natural radioactivity depends upon the geology of the region (Zheng et al., 2007; Rohit and Bala, 2014). A knowledge of both the concentration of naturally occurring radionuclides and the distribution of such radionuclides within geological materials is useful in order to evaluate dose rates and to

E-mail: Walharbi@kau.edu.sa. Tel: ++966564636265. Fax: +126063522-2427.

Figure 1. Location of iron ore samples collected from Wadi Sawawin.

establish reference data, which, in turn, play an important role in environmental radiation protection (Todorovic et al., 2015).

The aims of this study, which was based in Wadi Sawawin, were: (i) to assess local radiological hazards, (ii) to determine the corresponding radiation external doses to humans that were associated with the presence of a selection of locally occurring natural radionuclides (^{226}Ra, ^{238}Th and ^{40}K) and (iii) to specify mineral constituents of the local iron ores and the elemental concentrations of aluminium, calcium, iron, potassium, magnesium, bismuth, lead, thorium and uranium in those ores.

MATERIALS AND METHODS

Sampling and measurements

Fifteen iron ore samples were collected from Wadi Sawawin. Each sample was selected randomly at 1 to 2 km intervals. The iron ore samples were ground and sieved using a 1 mm mesh in order to obtain a uniform grain size. The ground samples were dried at 110°C for 12 h in order to remove all moisture and then weighed. For radiometric analysis, each ground and weighed sample was stored in a sealed polyethylene Marinelli beaker and kept for four weeks in order to attain a secular equilibrium between the ^{226}Ra and ^{228}Ra nuclides, as well as their progenies, by preventing leakage of radon gas (Malczewski and Zaba, 2012; Bello et al., 2015).

Ten grams of each sample were analysed using a Bruker XR-D D8 Advance powder X-ray diffraction system (Bruker, USA) in order to determine the concentration of the following elements: aluminium, calcium, iron, potassium, magnesium, bismuth, lead, thorium and uranium. A further 10 gm of each sample was analysed using a PinAAcle 900F atomic absorption spectrometer (Perkin Elmer, MA, USA). Samples of volume 5 mL were analysed for radioactivity levels using a Hyper-Pure Germanium detector (HPGe) gamma spectrometer, p-type crystal; Genie 2000 Basic Spectroscopy Software (Canberra, USA) was used for data acquisition, display and analysis. The relative efficiency of the detector was 25% and the full width at half maximum (FWHM) at 1461 keV was 4.2 keV (Rajeshwari et al., 2014; Raghu et al., 2015; Shittu et al., 2015). The lowest limits of detection were determined to be 0.30±0.06, 0.26±0.04 and 1.71±0.05 Bq kg^{-1} for ^{226}Ra, ^{232}Th, and ^{40}K, respectively. Each measurement was performed for a time period of approximately 10 h. The system was calibrated using standard reference material from International Atomic Energy Agency. Background radiation was measured using the same methodology as for the radiation measurements for the samples (Badawy et al., 2015). The activity concentrations of ^{232}Th, ^{226}Ra and ^{40}K were specified by using the following obvious and explicit peaks: ^{232}Th (338.32, 911.21 and 968.97 keV of ^{228}Ac, 727.25 keV of ^{212}Pb and 583.02, 2614.48 keV of ^{208}Tl), ^{226}Ra (351.9 keV of ^{214}Pb; 609.3, 1120.3 and 1764 keV of ^{214}Bi) and ^{40}K 1460.83 keV) (Amin, 2012).

Calculations methodology

The natural radionuclide concentrations in the iron ore samples were determined using the following equation (Patra et al., 2006; Laith et al., 2015):

$$Activity\,(Bqkg^{-1}) = \frac{Net\ peak\ area}{Collection\ time \times Emission\ probability \times Efficiency\ of\ the\ \det ector} \quad (1)$$

Additionally, the radium-equivalent activity (Ra_{eq}), the air-absorbed dose rate (D), the annual effective dose rates (AEDR) and the external hazard index (H_{ex}) of the iron ore were calculated, as shown in (Equations 2 to 5), respectively (Beretka and Mathew, 1985):

$$R_{eq} = C_{Ra} + 1.43C_{Th} + 0.077C_K \quad (2)$$

$$D = 0.0417C_K + 0.462C_{Ra} + 0.604C_{Th} \quad (3)$$

Table 1. Average activity concentration of ^{226}Ra, ^{232}Th, ^{40}K in the iron ore used in this study.

Sample code	Average activity concentration (Bq kg^{-1})		
	^{226}Ra	^{232}Th	^{40}K
WD-1	2.18±0.30	1.21±0.16	2.40±0.36
WD-2	3.66±0.36	1.75±0.22	3.18±0.42
WD-3	2.92±0.36	1.32±0.17	2.79±0.13
WD-4	3.79±0.44	1.92±0.28	4.08±0.98
WD-5	4.11±0.64	1.74±0.30	DL
WD-6	3.65±0.53	1.65±0.24	5.03±1.05
WD-7	1.89±0.39	3.60±0.56	2.72±0.51
WD-8	3.21±0.39	1.88±0.29	DL
WD-9	3.40±0.27	1.65±0.43	DL
WD-10	3.73±0.50	1.61±0.25	4.28±1.01
WD-11	3.75±0.57	1.74±0.24	2.20±0.50
WD-12	3.71±0.42	3.57±0.48	10.33±1.32
WD-13	4.50±0.53	1.86±0.31	5.23±0.75
WD-14	3.68±0.41	2.51±0.31	7.69±1.01
WD-15	4.20±0.41	2.72±0.30	7.80±0.81

DL: detection limit.

$$AEDR = D \times 24h \times 365days \times 0.2 \times 0.7 \times 10^{-6} \quad (4)$$

$$H_{ex} = \frac{C_{Ra}}{370} + \frac{C_{Th}}{259} + \frac{C_K}{4810} \leq 1 \quad (5)$$

In Equations 2, 3 and 4, the terms C_{Ra}, C_{Th} and C_K are average activity concentrations of ^{226}Ra, ^{232}Th and ^{40}K, respectively. The measured activity was converted into doses using the following conversion factors: 0.0414 nGy h^{-1} per Bq kg^{-1} for ^{40}K, 0.461 nGy h^{-1} per Bq kg^{-1} for ^{226}Ra, and 0.623 nGy h^{-1} per Bq kg^{-1} for ^{232}Th. In Equation 4, the number 0.7 is a conversion factor and 0.8 is the outdoor occupancy factor for when most people spend 20% of their time indoors.

RESULTS AND DISCUSSION

Natural radioactivity determination

The average radionuclide activity concentrations in the iron ore samples varied from 1.89±0.39 to 4.50±0.53 Bq kg^{-1}, from 1.21±0.16 to 3.60±0.56 Bq kg^{-1}, and from the detection limit (DL) to 10.33±1.32 Bq kg^{-1} for ^{226}Ra, ^{232}Th and ^{40}K, respectively, as detailed in Table 1. All measurements fell below the manufacturer recommended values of 35, 30 and 400 Bq kg^{-1} for ^{226}Ra, ^{232}Th and ^{40}K, respectively (UNSCEAR, 1993).

The Ra_{eq} of the iron ores varied between 2.36 and 9.61 Bq kg^{-1}, as detailed in Table 2. The Ra_{eq} values were below the recommended level of 370 Bq kg^{-1} for building material and its products (NEA/OECD-Nuclear Energy Agency, 1979). The absorbed dose rate D was determined in the range of 1.00 to 4.30 nGy h^{-1}. The maximum value of D less than permissible limit (84nGy h^{-1}) according to UNSCEAR (2000). The AEDR was within the range 0.001 to 0.005 mSv y^{-1}, indicating that the AEDR is within the 0.3 to 1.0 mSv y^{-1} range recommended by the OECD/NEA-Nuclear Energy Agency (1979). The H_{ex} values of the iron ore samples were also calculated and they ranged from 0.01 and 0.03, as shown in Table 2. For the safe use of a material in the construction of dwellings, it is proposed that H_{ex} should be less than unity (Beretka and Mathew, 1985). Figure 2 shows the average radionuclide activity concentrations in the iron ore samples, while Figures 3, 4, 5 and 6 show the parameters of the radiological hazards: Ra_{eq},D, AEDR and H_{ex}, respectively. Therefore, iron ore from the region studied here is radiologically safe to be used as a construction material without posing any significant radiological risk to users or the general populations (Faanu et al., 2011).

Malczewski and Zaba (2012) determined uranium, thorium and potassium concentrations in rocks obtained from the Modane-Aussois region of France (Western Alps) using HPGe. Their results revealed that the activity concentration of ^{238}U ranged from 9 Bq kg^{-1} (quartzite) to 29 Bq kg^{-1} (dolomite). Furthermore, in that study, the highest activity concentrations that were associated with ^{232}Th and ^{40}K were measured in calcschist and in quartzite (18 Bq kg^{-1} and 572 Bq kg^{-1}, respectively). Akkurt and Günoglu (2014) evaluated the radioactivity levels of ^{40}H, ^{232}Th and ^{238}Ra in sedimentary rock obtained from Turkey, where they found that the mean activities were below the recommended values identified by UNSCEAR(2000). In that study, the calculated average values of Ra_{eq}, D, AEDT and H_{ex} were 99.0 Bq kg^{-1}, 45.43 nGy h^{-1} , 0.056mSv y^{-1} and 0.27, respectively. All measurements were lower than the global maximum values reported by UNSCEAR (2000).

Table 2. Radiologic hazard effects D, AEDE, Ra_{eq} and H_{ex} of the iron ore used in this study.

Sample code	D (nGy h^{-1})	AEDE ($mSvy^{-1}$)	Ra_{eq} (Bq kg^{-1})	H_{ex}
WD-1	1.83	0.002	4.09	0.01
WD-2	2.88	0.004	6.41	0.02
WD-3	2.26	0.003	5.02	0.02
WD-4	3.08	0.004	6.85	0.02
WD-5	3.01	0.004	6.71	0.02
WD-6	2.90	0.004	6.40	0.02
WD-7	2.77	0.004	6.23	0.02
WD-8	2.68	0.003	6.01	0.02
WD-9	1.00	0.001	2.36	0.01
WD-10	2.87	0.004	6.36	0.02
WD-11	2.88	0.004	6.41	0.02
WD-12	4.30	0.005	9.61	0.03
WD-13	3.48	0.004	7.70	0.02
WD-14	3.54	0.004	7.86	0.03
WD-15	3.90	0.005	8.69	0.03

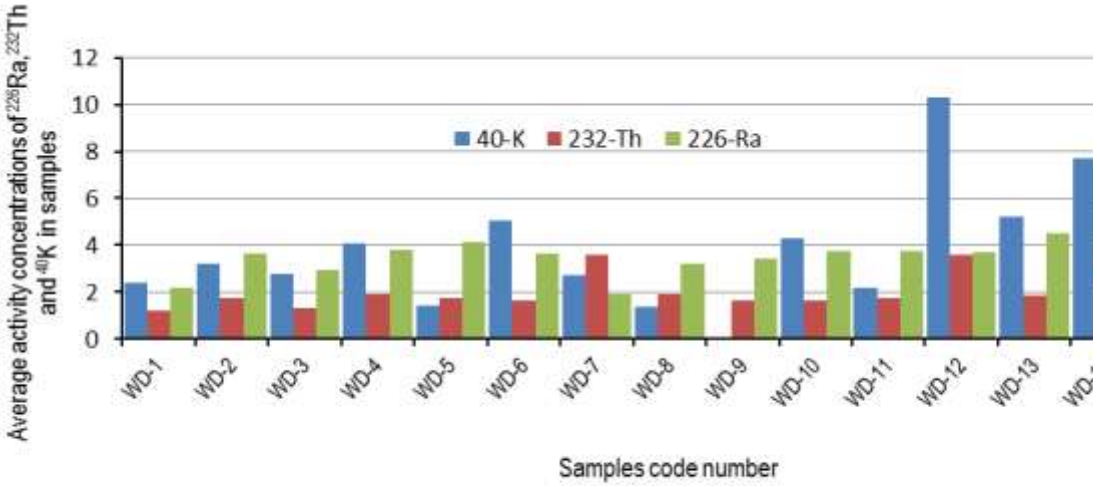

Figure 2. Average activity concentration of ^{226}Ra, ^{232}Th and ^{40}K in Iron ore sample.

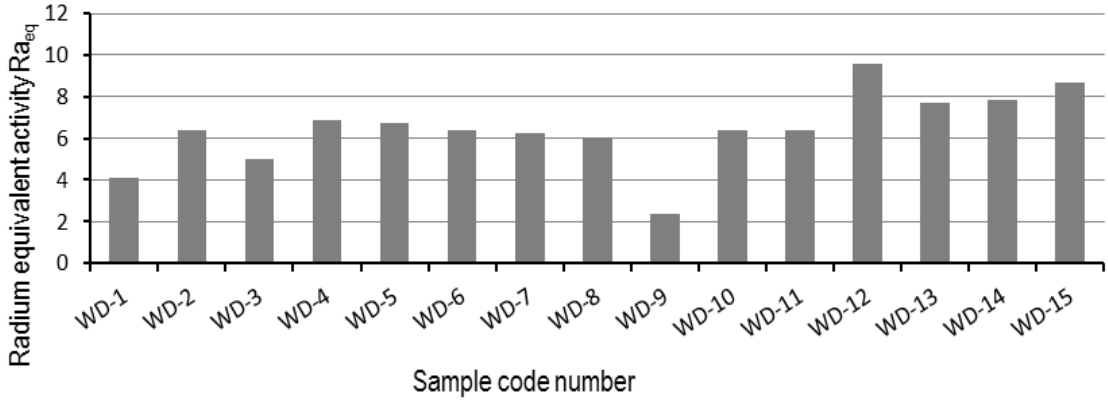

Figure 3. The parameter of the radiological hazard: Radium equivalent activity Ra_{eq} in $Bqkg^{-1}$.

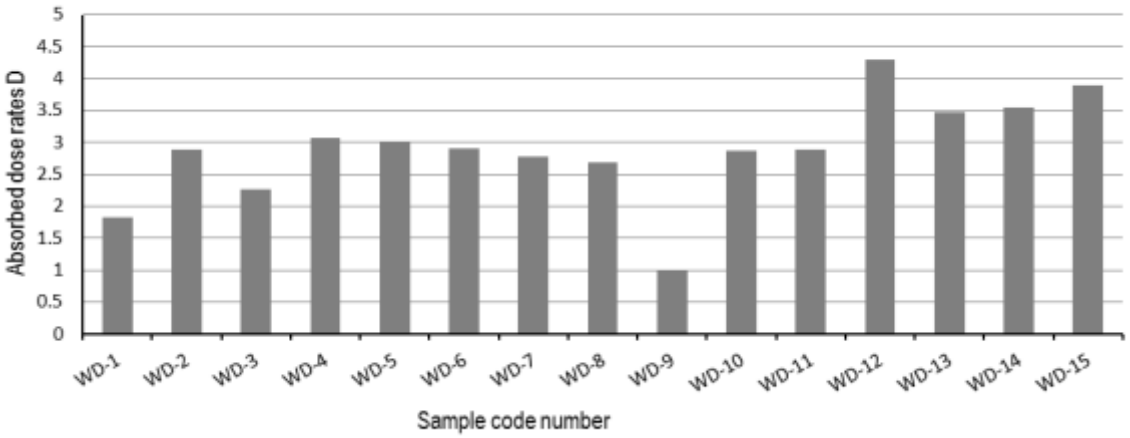

Figure 4. The parameter of the radiological hazard: Absorbed dose rates D in $nGyh^{-1}$.

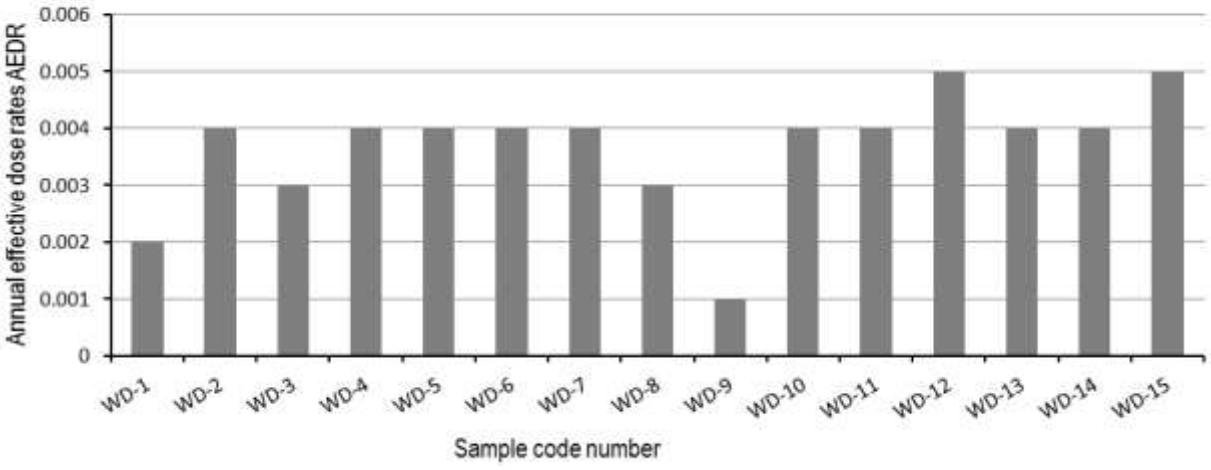

Figure 5. The parameter of the radiological hazard: Annual effective dose rates AEDR in $mSvy^{-1}$.

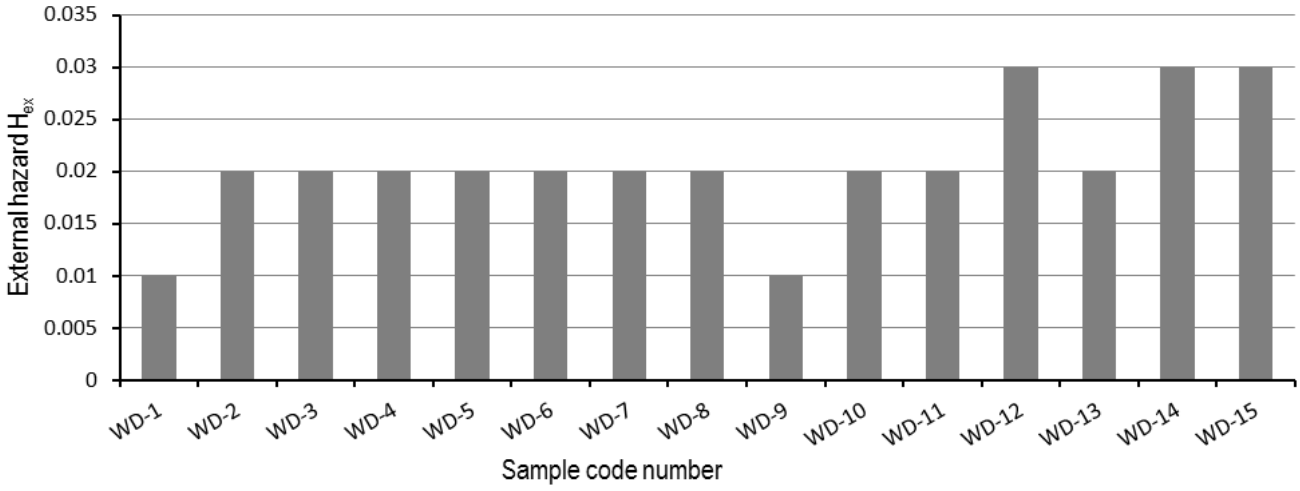

Figure 6. The parameter of the radiological hazard: External hazard H_{ex}.

Table 3. Mean elemental concentrations determined using an atomic absorption spectrometer analyser.

Element	Al	Ca	Fe	K	Mg	Bi	Pb	Th	U
unit	%	%	%	%	%	ppm	ppm	ppm	ppm
DL	**0.02**	**0.02**	**0.01**	**0.01**	**0.01**	**10.00**	**2.00**	**1.00**	**5.00**
WD-1	0.10	3.79	38.85	DL	0.35	BDL	14.29	1.27	BDL
WD-2	0.20	3.23	54.69	DL	0.12	BDL	4.79	2.97	BDL
WD-3	0.15	3.52	47.01	DL	0.24	BDL	9.54	2.12	BDL
WD-4	0.18	2.96	45.05	DL	0.13	BDL	7.06	2.09	BDL
WD-5	0.17	3.50	55.97	DL	0.16	BDL	BDL	1.96	BDL
WD-6	0.20	2.95	60.99	DL	0.13	BDL	BDL	2.01	BDL
WD-7	0.13	2.20	48.27	BDL	0.07	BDL	7.78	BDL	BDL
WD-8	0.19	2.61	47.10	DL	0.12	BDL	5.10	1.23	BDL
WD-9	0.24	2.97	45.86	DL	0.17	BDL	2.29	1.51	BDL
WD-10	0.14	2.52	48.45	DL	0.08	BDL	2.96	1.54	BDL
WD-11	0.19	2.75	47.20	DL	0.13	BDL	2.70	1.53	BDL
WD-12	0.19	2.36	61.43	DL	0.09	BDL	2.81	1.07	BDL
WD-13	0.15	3.38	58.25	DL	0.12	BDL	BDL	2.27	BDL
WD-14	0.19	2.71	61.21	DL	0.11	BDL	BDL	1.60	BDL
WD-15	0.17	2.90	59.85	DL	0.21	BDL	2.30	1.70	BDL

BDL: Below detection limit.

Atomic Absorption Spectrometer (AAS) analytical results

Table 3 details the elemental concentrations of the iron ore samples as measured by an atomic absorption spectrometer (Popescu et al., 2009; El-Taher, 2010). The (DL) values for U, Th, Pb, Bi, Mg, K, Fe, Ca and Al were 5, 1, 2, 10, 100, 100, 100, 200 and 200 ppm, respectively. Potassium, bismuth and uranium concentrations were below detection limit (BDL). Lead was detected in all samples except for WD-5, WD-6, WD-13 and WD-14, and it varied from (BDL) to 14.29 ppm and from (BDL) to 2.97 ppm for thorium. Thorium was not detected in sample WD-7. The concentrations of aluminium, calcium, iron and magnesium were measured to be in the following ranges: 0.10 to 0.24% for aluminium, 2.2 to 3.790% for calcium, 38.85 to 61.43% for Iron and 0.07 to 0.35% for magnesium. The concentration of potassium was at, or lower than (DL).

Papastergios et al. (2004) used inductively coupled plasma optical emission spectrometry (ICP-OES) and inductively coupled plasma mass spectrometry (ICP-MS) to measure the concentration of the following elements in uncultivated top-soils and various surrounding rocks: calcium, magnesium, potassium, boron, strontium, iron, sodium, silicon, sulphur, aluminium, zinc, manganese, titanium, copper, vanadium, rubidium, chromium, barium, bismuth, lanthanum, thorium, cerium, tin, arsenic, cobalt, yttrium, selenium, zircon, cadmium, molybdenum, caesium, antimony, tungsten, uranium, lithium, silver, mercury, nickel, germanium and lead. The results of the study by Papastergios et al. (2004) showed that the concentrations of elements in the topsoil were influenced mainly by their concentration in surrounding rocks. Mean trace element concentrations in the topsoil were compared with the global average values for Fluvisol and Leptosol soil types (FAO, 1974; Kabata-Pendias, 2011). Moreover, the topsoil mean trace element concentrations were compared with those from three surrounding rock samples; it was found that all the samples had high concentrations of aluminium and iron, while magnesium, calcium, thorium, and lead were in the range of safe concentrations in all the samples except WD-1 and WD-15.

The UK deems a safe maximum concentration for lead in soil to be 300 mg kg^{-1}, whereas in most countries it is deemed to be 100 mg kg^{-1} (Kabata-Pendias, 2011). Fergusson (1990) found that some ferritic soils have bismuth concentrations of up to 10 mg kg^{-1}, whereas Tyler and Olsson (2005) found bismuth concentrations of 92 mg kg^{-1} in raw humus soil.

X-ray diffraction: Analytical results

Table 4 details the mineral content and description of fifteen iron ore samples obtained by X-ray diffraction (Preeti and Singh, 2007; Srivastava, 2014). The trace mineral calcite ($CaCO_3$) was monitored and found to be present in all samples. The major minerals quartz (SiO_2), haematite (Fe_2O_3) and titanium III oxide (Ti_2O_3) were detected in samples WD-1, WD-2, WD-3, WD-4 and WD-5, while for the remaining samples, only quartz (SiO_2), haematite (Fe_2O_3) were detected.

Table 4. Minerals contents by XRD.

Sample code	Major mineral	Trace mineral
WD-1	Quartz {SiO_2}, Haematite {Fe_2O_3}, Titanium{$Fe(0.927)Ti(0.073))_2O_3$}	Calcite {$CaCO_3$}
WD-2	Quartz {SiO_2}, Haematite {Fe_2O_3}, Titanium{$(Fe(0.927)Ti(0.073))_2O_3$}	Calcite {$CaCO_3$}
WD-3	Quartz {SiO_2}, Haematite {Fe_2O_3}, Titanium{$(Fe(0.927)Ti(0.073))_2O_3$}	Calcite {$CaCO_3$}
WD-4	Quartz {SiO_2}, Haematite {Fe_2O_3}, Titanium{$(Fe(1.831)Ti(0.169))_2O_3$}	Calcite {$CaCO_3$}
WD-5	Haematite {Fe_2O_3}, Titanium{$(Fe(0.927)Ti(0.073))_2O_3$}, Quartz {$SiO_2$}	Calcite {$CaCO_3$}
WD-6	Haematite {Fe_2O_3}, Quartz {SiO_2}	Calcite {$CaCO_3$}
WD-7	Quartz {SiO_2}, Haematite {Fe_2O_3}	Calcite {$CaCO_3$}
WD-8	Quartz {SiO_2}, Haematite {Fe_2O_3}	Calcite {$CaCO_3$}
WD-9	Quartz {SiO_2}, Haematite {Fe_2O_3}	Calcite {$CaCO_3$}
WD-10	Quartz {SiO_2}, Haematite {Fe_2O_3}	Calcite {$CaCO_3$}
WD-11	Quartz {SiO_2}, Haematite {Fe_2O_3}	Calcite {$CaCO_3$}
WD-12	Haematite {Fe_2O_3},Quartz {SiO_2}	Calcite {$CaCO_3$}
WD-13	Haematite {Fe_2O_3},Quartz {SiO_2}	Calcite {$CaCO_3$}
WD-14	Haematite {Fe_2O_3},Quartz {SiO_2}	Calcite {$CaCO_3$}
WD-15	Haematite {Fe_2O_3},Quartz {SiO_2}	Calcite {$CaCO_3$}

Haematite is one of the most abundant minerals found on the surface and in the shallow crust of the Earth's surface, being found in sedimentary, metamorphic and igneous rocks at locations throughout the world. Haematite's colour ranges from black to grey and from red to brown. Haematite has played an important economic role in human society as a primary source of iron. Rust is simply another form of haematite and haematite dust is responsible for the reddish colour of many soils and the Martian landscape (Kormann et al., 1989; Deer et al., 2013).

Cevika et al. (2010) investigated the structure, chemical characterisation and radiological properties of phosphate rock from Turkey using X-ray fluorescence, X-ray diffraction and an HPGe detector, and they compared the data to results obtained from several studies on phosphate rocks from Egypt, Syria, Tunisia, Algeria, and Morocco. The mineral analysis showed that phosphate samples were composed of P_2O_5, CaO, SiO_2, SO_3, Fe_2O_3, Al_2O_3 and TiO_2. The mean activity concentrations of ^{226}Ra, ^{232}Th and ^{40}K in the phosphate samples were 535, 20 and 148 Bq kg^{-1}, respectively. The radiological hazard was also assessed. The average of absorbed dose rate in air D, AEDE and Ra_{eq} were in the same range as reported for the individual countries and worldwide for all phosphate samples.

Conclusions

To evaluate the human health risk in Wadi Sawawin, in the Duba region of Saudi Arabia, the background radiation levels were determined using HPGe detector. The results reveal that the average activity concentration of ^{40}K,^{232}Th and ^{226}Ra in all Iron ore rocks samples are lower than their corresponding allowed limit according to the worldwide values. Also, all the calculated values of radiological hazard are within the permissible range reported by UNSCEAR (2000). So, it can be concluded that the region under study is safe for inhabitation. In addition, the elemental concentrations Al, Ca, Fe, K, Mg, Bi, Pb, Th and U in the iron ore samples as measured by an atomic absorption spectrometer. Also, the mineral content was determined using X-ray diffraction, quartz (SiO_2) and haematite (Fe_2O_3) were detected in all samples as minor mineral content, while the Calcite $CaCO_3$ was monitored in all samples as a trace mineral content. Finally, Iron ore extracted from the region under study can be used as building material.

Conflict of Interests

The authors have not declared any conflict of interests.

REFERENCES

Akkurt I, Günoglu K (2014). Natural radioactivity measurements and radiation dose estimation in some sedimentary rock samples in Turkey. Sci. Technol. Nucl. Ins. 1-6.

Amin RM (2012). Gamma radiation measurements of naturally occurring radioactive samples from commercial Egyptian granites. Environ. Earth Sci. 67:771-775.

Badawy WM, El-kameesy SU, Soliman NF, Eissa HS, Mahmoud AW (2015). Natural radioactivity and the associated dose from the terrestrial ecosystem of Ismailia Canal, Egypt. Int. J. Adv. Res. 3(1):768-778.

Bello IA, Najib MU, Umar SA, Ibrahim GG (2015). Measurement of natural radioactivity concentration at E-waste dumpsite around Alaba international market Lagos, Nigeria. Adv. Appl. Sci. Res. 6(6):55-64.

Beretka J, Mathew PJ (1985). Natural radioactivity of Australian building materials, industrial wastes and by-products.Health Phys. 1:87-95.

Cevika U, Baltasb H, Tabakc A (2010). Damlad, N. Radiological and

chemical assessment of phosphate rocks in some countries. J. Hazard. Mater. 182:531-535.
Deer WA, Howie RA, Zussman J (1992). 3rd ed. An introduction to the rock-forming minerals. London: Mineralogical Society.
El-Taher A (2010). Elemental analysis of two Egyptian phosphate rock mines by instrumental neutron activation analysis and atomic absorption spectrometry. Appl. Radiat. Isot. 68:511-515.
Faanu A, Ephraim JH, Darko EO (2011). Assessment of public exposure to naturally occurring radioactive materials from mining and mineral processing activities of Tarkwa Goldmine in Ghana. Environ. Monit. Assess. 180(1-4):15-29.
Fergusson JE (1990). The heavy metals: chemistry, environmental impact and health effects. Pergamon Press, New York
Food and Agriculture Organization of the United Nations (FAO) (1974). Legend of the soil map of the world. Unesco – Paris.
Kabata-Pendias A (2011). Trace elements in soils and plants, 4th ed. Taylor & Francis: London, New York
Kormann C, Detlef WB, Michael RH (1989). Environmental photochemistry: Is iron oxide (hematite) an active photocatalyst? A comparative study: α-Fe2O3, ZnO, TiO_2. J. Photochem. Photobiol. A. 48(1):161-169.
Laith AN, Younis SA, Kithah FH (2015). Natural radioactivity in soil samples in Nineveh Province and the associated radiation hazards. Int. J. Phys. 3(3):126-132.
Malczewski D, Żaba J (2012). Natural radioactivity in rocks of the Modane–Aussois region (SE France). J. radioanal. Nucl. Chem. 292(1):123-130.
Nuclear Energy Agency of the OECD (NEA/OECD) (1979). Recommended Operational Procedure for Sea Dumping of Radioactive Waste, Paris.
Patra AK, Sudhakar J, Ravi PM, James JP, Hegde AG, Joshi ML (2006). Natural radioactivity distribution in geological matrices around Kaiga environ. J. Radioanal. Nucl. Chem. 270(2):307-312.
Papastergios G, Georgakopoulos A, Fernandez-Turiel JL, Gimeno D, Filippidis A, Kassoli-Fournaraki A, Grigoriadou A (2004). Heavy metals and toxic trace elements contents in selected areas of the Kavala Prefecture, Northern Greece. Bull. Geol. Soc. Greece, 36(1):263-272.
Popescu IV, Stihi C, Cimpoca GHV, Dima G, Vlaicu GH, Gheboian A, Bancuta I, Ghisa V, State G (2009).Environmental samples analysis by atomic absorption spectrometry (AAS) and inductivity coupled plasma-optical emission spectroscopy (ICP-AES). Rom. J. Phys. 54(7-8):741-746.
Preeti SN, Singh BK (2007). Instrumental characterization of clay by XRF, XRD and FTIR. Bull. Mater. Sci. 30(3):235-238.
Rajeshwari T, Rajesh S, Kerur BR, Anilkumar S, Krishnan N, Pant AD (2014). Natural radioactivity studies of Bidar soil samples using gamma spectrometry. J. Radioanal. Nucl. Chem. 300:61-65.
Raghu Y, Harikrishnanm N, Chandrasekaran A, Govardhanan B, Ravisankar R (2015). FFA Study on activity concentration of Nntural radionuclides of building materials in Pachal, Tiruvannamalai dist. Tamilnadu, India. J. Environ. Health Sci. pp. 1-5.
Rohit M, Bala P (2014). Assessment of radiation hazards due to the concentration of natural radionuclides in the environment. Environ. Earth Sci. 71:901-909.
Shittu HO, Olarinoye IO, Baba-Kutigi AN, Olukotun SF, Ojo EO, Egga A (2015). Determination of the radiological risk associated with naturally occurring radioactive materials (NORM) at selected quarry sites in Abuja FCT, Nigeria: using gamma-ray spectroscopy. Phys. J. 1(2):71-78.
Srivastava A, Swain KK, Vashisht B, Aggarwal P, Mete U, Acharya R, Wagh DN, Reddy AVR (2014). Studies of kidney stones using INAA, EDXRF and XRD techniques. J. Radioanal. Nucl. Chem. 300:191-194.
Todorovic N, Bikit I, Krmar M, Mrdja D, Hansman J, Nikolov J, Forkapic S, Veskovic M, Bikit K, Jakoni I (2015). Natural radioactivity in raw materials used in building industry in Serbia. Int. J. Environ. Sci. Technol. 12:705-716.
Tyler G, Olsson T (2005). Rare earth elements in forest-floor herbs as related to soil conditions and mineral nutrition. Biol. Trace Elem. Res. 106:177-191.
United Nations Scientific Committee on the Effects of Atomic Radiation (UNSCEAR) Annex A (1993): Exposure from Natural Sources, United Nations, NY, USA.
United Nations Scientific Committee on the Effects of Atomic Radiation (UNSCEAR) Annex A (2000): Exposure from Natural Sources, United Nations, New York, NY, USA.
Zheng G, Lang Y, Miyahara M, Nozaki T, Haruaki T (2007). Iron oxide precipitate in seepage of groundwater from a landslide slip zone. Environ. Geol. 51:1455-1464.